Headline Articles

Ultrafast Photochemistry of Ammonia Clusters: Formation and Decay of Hypervalent Molecular Clusters Containing the NH_4 Radical

Kiyokazu Fuke*,# and Ryozo Takasu

Institute for Molecular Science, Myodaiji, Okazaki 444
The Graduate University for Advanced Studies, Myodaiji, Okazaki 444

(Received August 9, 1995)

The photochemical reaction of ammonia clusters in the first excited state was studied by a femtosecond pump-probe technique and time-of-flight mass spectroscopy. Small ammonia clusters containing the NH_4 radical were probed by a resonance enhanced two-photon ionization method. The NH_4 radical is formed within 0.5 ps, and decomposes with a lifetime of 13 ps. The ammonia dimer ion was found to be formed mainly through the one-photon ionization of a new photolysis product such as an excited-state NH_4*–NH_2. This intermediate may correspond to a cage product in the predissociation process of larger ammonia clusters; its formation and decay times are ca. 1 ps and <1 ns, respectively. We also examined the lifetimes of $NH_4(NH_3)_n$ using the pump-probe technique with nanosecond lasers. The lifetime of NH_4 was found to be elongated by more than 10^6 times in ammonia clusters. The mechanism of the formation and decay processes for these species as well as for the resonance-enhanced two-photon ionization of ammonia clusters were discussed on the basis of the present results in conjunction with theoretical results from literature.

The photoionization process of ammonia clusters has been one of the central issues in cluster research for the last two decades.[1] The ionization mechanism has been extensively studied using various ionization techniques, including electron impact,[2,3] single-photon[4—6] and multiphoton ionization.[7—10] Protonated cluster ions, $(NH_3)_nH^+$, were found to be produced dominantly by the former two processes. In these processes, the direct ionization of $(NH_3)_n$ generates $(NH_3)_n^+$, which are unstable, and are followed by a proton-transfer reaction to form $NH_4^+(NH_3)_{n-2}$ including a loss of NH_2. The latter reaction was also studied in detail by ab initio calculations.[11—13] The resonance-enhanced two-photon ionization (RE2PI) of clusters through the first singlet electronic state (A^1A_2'') of the ammonia molecule has also been examined. Kassab and co-workers theoretically predicted a mechanism for the production of $NH_4^+(NH_3)_n$ through the ionization of $NH_4(NH_3)_n$.[12] Since the A-state ammonia is predissociative ($NH_3 \rightarrow NH_2 + H$, lifetime < 200 fs),[14,15] $NH_4(NH_3)_n$ is expected to be formed efficiently through an intracluster reaction. This process may compete with the ionization of $(NH_3)_n$* by the second photon, which is followed by a reaction in the ionization state to produce protonated cluster ions. Recently, these two mechanisms to produce $NH_4^+(NH_3)_n$ were experimentally confirmed using nanosecond[9,10] and femtosecond pump-probe techniques.[16,17] Although these studies revealed the photoionization process of $(NH_3)_n$ via the A state, our understanding of the predissociation process still seems to be incomplete; only the process to produce $NH_4(NH_3)_m$, involving a concomitant NH_2 loss, has been determined. These results raise an interesting question as to whether a cluster containing the NH_2 radical is formed or not in the molecular beam after photolysis. This issue seems to be quite important in order to fully understand the photochemistry of $(NH_3)_n$ on the A-state surface as well as the mechanism for the RE2PI of $(NH_3)_n$.

As mentioned above, the clusters containing the NH_4 radical are the key species in the RE2PI of ammonia clusters. This radical has also been considered to be an important intermediate in solution chemistry. The possible existence of the NH_4 radical in the reaction of the solvated electron and in electrochemistry has

#Present address: Department of Chemistry, Kobe University, Nada-ku, Kobe 657.

been speculated on for many years.[18—21] The spectroscopic properties of NH_4 have been studied extensively since the first spectroscopic characterization by Herzberg.[22,23] According to these studies, NH_4 has a very shallow potential well in the ground state, and, as a result, has a short lifetime. Porter and co-workers have studied the stability of small $NH_4(NH_3)_n$ by a neutralized ion beam technique, and found that the radical is extensively stabilized by complex formation with ammonia.[24—26] Recently, the structure and stability of ammoniated NH_4 radical were also investigated theoretically by Kassab and co-workers.[12,27] We also examined the ionization potentials of ammoniated NH_4 clusters in relation to an electron localization mode in gas-phase clusters.[28] However, the experimental data concerning the physical and chemical properties of ammoniated NH_4 are still quite limited. A study on the stability of these clusters as a function of the number of solvent molecules may provide a clue regarding the long-standing problems in bulk solution.

In the present work we studied the formation and decay processes of ammoniated NH_4 clusters produced by the photolysis of jet-cooled $(NH_3)_n$ using nano- and femtosecond pump-probe techniques. The pump-probe curves for $NH_4^+(NH_3)_n$, n=0—4, present multiple decay components corresponding to the predissociation of the A-state ammonia molecule and solvation of the NH_4 radical in clusters. As has been reported previously, unprotonated ammonia cluster ions, $(NH_3)_n^+$, were rarely observed, except for n=1 and 2. The curve for $(NH_3)_2^+$ was found to exhibit a clear rising feature with a time constant of a few ps. This ion is formed by the one-photon ionization of a new intermediate having an ionization threshold of 3.79 eV. From a comparison of these results and theoretical predictions, we assigned the intermediate as being an excited-state NH_4^*–NH_2; a cage product of the intracluster reaction, and the final ionic state has the form of $NH_4^+NH_2$. We also examined the lifetime of $NH_4(NH_3)_n$, n=0—5. On the basis of these results, we discuss the predissociation process of ammonia clusters in the first excited state, and the formation and decomposition processes of the produced clusters containing the NH_4 radical.

Experimental

Details concerning the experimental apparatus used in the present study have been described elsewhere.[29] The system consists of a three-stage differentially evacuated chamber which includes a cluster source and a reflectron-type time-of-flight (TOF) mass spectrometer. The ammonia clusters were generated by the supersonic expansion of pure ammonia (4 atm) from a pulsed nozzle (General valve, series 9). Figure 1 shows the setup for the femtosecond pump-probe experiment. Femtosecond laser pulses were generated by a Ti-sapphire laser (Spectra Physics, Tsunami). The output was amplified by a regenerative amplifier pumped by a 10 Hz Nd:YAG laser (Quanta-Ray, GCR-150). The output wavelength, pulse width, and energy were ca. 789 nm, 120 fs and

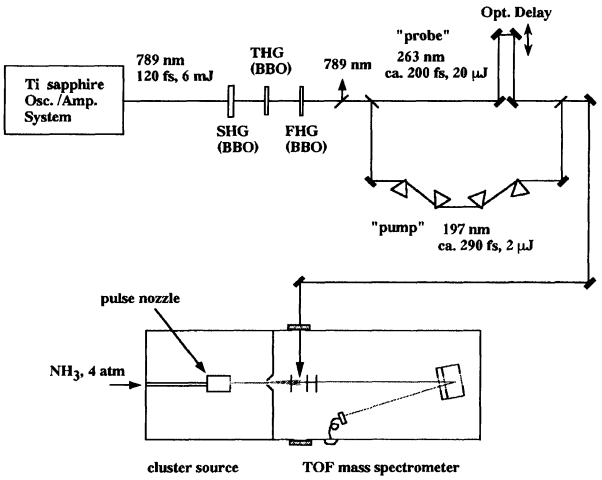

Fig. 1. Setup for femtosecond pump-probe experiments of ammonia clusters.

6 mJ/pulse, respectively. The pump pulses near to 197 nm were generated by a phase-matched sequential conversion of the 789 nm pulse in three BBO crystals arranged in a nonlinear sum-frequency mixing scheme. The energy of the pump pulses was typically 2 μJ/pulse. The pulse duration of the pump pulses was measured by a down-conversion with the pulse at the fundamental. A cross-correlation trace at a signal wavelength of 263 nm gave a full width at half-maximum (FWHM) of about 360 fs. Assuming a sech^2 pulse, the deconvolution led to a pump pulse width of 290 fs. The third harmonic at 263 nm (ca. 20 μJ/pulse) was used as the probe pulses. The pump and probe pulses were separated by a 45° reflecting mirror; the latter pulses were sent through a delay stage. Thereafter, both pulses were recombined using another 45° high reflector. The laser beams were then introduced into the interaction region without focusing, where they intersected the cluster beam. Cluster ions produced by two femtosecond pulses were accelerated and introduced to the field-free region of the reflectron TOF mass spectrometer. The ions were reflected by electric fields at the end of the TOF chamber, and were detected by dual microchannel plates (Hamamatsu, F1552-23S) after flying back into the field-free region. The output signals were fed into a digital storage oscilloscope (LeCroy 9450) after being amplified by a wide-band amplifier (NF Electronic Instruments, BX-31). The mass spectra were measured at various delay times between the pump and probe pulses.

The lifetimes of $NH_4(NH_3)_n$ ($1 \leq n \leq 5$) were examined by pump-probe experiments using nanosecond lasers. An ArF excimer laser (Lambda Physik, COMPex) was used as the pump laser; a laser beam of ca. 100 μJ/pulse and 1-mm diameter was used without focusing. A far-field beam of a XeCl laser (Lambda Physik, LPX205) at 308 nm was used as the probe laser. In order to suppress the loss of the $NH_4(NH_3)_n$ clusters from the ionization region, a probe beam with a large cross section (5 mm height and 15 mm width) and an ArF laser beam were introduced colinearly and counterpropergatedly to the acceleration region of the mass spectrometer, as mentioned later. The lifetime was measured by detecting the ion signals as a function of the delay time between the pump and the probe pulses.

The ammonia (NH_3, minimum purity of 99.99%, Nippon

Sanso) was used without further purification.

Results

Figure 2 shows the typical TOF mass spectra of protonated, $NH_4^+(NH_3)_n$, and unprotonated, $(NH_3)_n^+$, ammonia cluster ions produced by two femtosecond laser photons with various delay times. The pump wavelength at 197 nm corresponds to the excitation of an ammonia molecule to the $v_2'=5$ bending vibrational level in the A^1A_2'' state, while the probe pulse is at 263 nm. Since the ion signals were found to be easily saturated by the pump laser pulses (>10 μJ/pulse) alone, the laser intensity was attenuated to less than 5 μJ/pulse. Protonated ions were detected dominantly in the time region examined, while the unprotonated ions, except for $n=1$ and 2, were weakly observed at the time when two pulses temporally overlapped.

Figure 3 shows the pump-probe curves for the small ammonia cluster ions through the A ($v_2'=5$) state with a time step of 83 fs. These curves were obtained by averaging the results of several pump-probe experiments under the same conditions. The curve for the NH_3^+ ion shown in Fig. 3a exhibits a sharp spike with a FWHM of 370 fs. The temporal profile is symmetrical with respect to the delay times between the pump and probe pulses; the base line is also at the same level for both edges. The width of the spike is nearly the same as that for the cross-correlation function of the pump and probe pulses; the NH_3^+ ion signals give approximately a time-response function of the experimental system. Thus, the zero of the time is defined at the peak of the NH_3^+ ion signals.

As can be seen in Fig. 3b, the peak of the NH_4^+ ion signals is delayed by about 200 fs with respect to that for NH_3^+. The curve exhibits the fast and slow decay components; the features are clearly seen in the pump-probe curve with a longer delay time, as

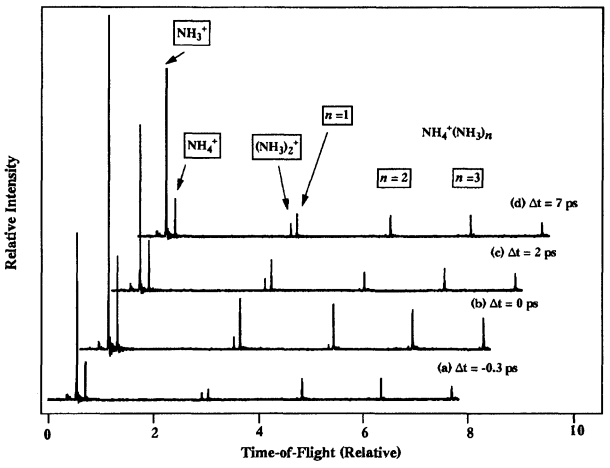

Fig. 2. Typical TOF mass spectra of small ammonia cluster ions generated by two femtosecond laser pulses with various delay times; pump pulses at 197 nm, A ($v_2'=5$), and probe pulses at 263 nm.

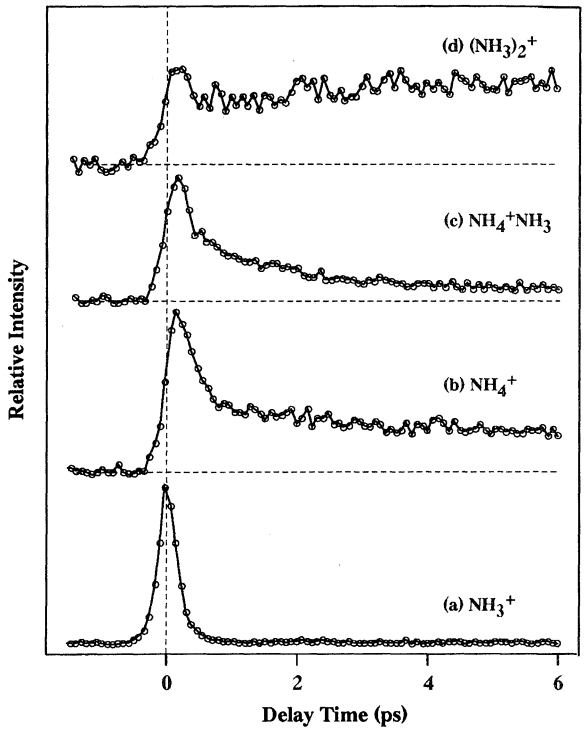

Fig. 3. Pump-probe curves of NH_3^+ (a), NH_4^+ (b), $NH_4^+NH_3$ (c), and $(NH_3)_2^+$ (d) with a scan step of 83 fs; pump pulses at 197 nm, A ($v_2'=5$), and probe pulses at 263 nm. The signals, at the time when the probe is ahead of the pump, are the background ion signals from one color ionization by the pump laser alone.

shown in Fig. 4b. The energy of the probe laser at 263 nm (4.71 eV) is well above the ionization energy of the excited-state ammonia clusters (ca. 3.9 eV),[4] and also exceeds the ionization threshold of the NH_4 radical (4.62 eV).[28] Thus, these ions are considered to be formed through the photoionization of excited-state ammonia clusters, followed by the proton-transfer reaction [absorption–ionization–dissociation (AID) mechanism] as well as the photoionization of NH_4 produced by the intracluster reaction [absorption–dissociation–ionization (ADI) mechanism]. Although the pump-probe curve of $NH_4^+(NH_3)$ also shows fast and slow decay components, the decay of the latter component is seen to be faster than that for NH_4^+. The pump-probe curves of $NH_4^+(NH_3)_n$ ($n=2$—4) also display two components (Fig. 5). These results seem to indicate that the decay time for the slow component becomes longer with increasing n. Recently, the formation of $NH_4^+(NH_3)_n$ ($n=1$—4) through the A ($v_2'=0$—2) states was also examined by Castleman and co-workers;[16,17] the major features that they reported are consistent with the present results. These observations suggest that the origin of the slow component of NH_4^+ is different from those for $n\geq1$. According to the aforementioned spectroscopic studies, NH_4 decomposes with a lifetime of less than 100 ps.[22,23] Thus, the slow-decay component

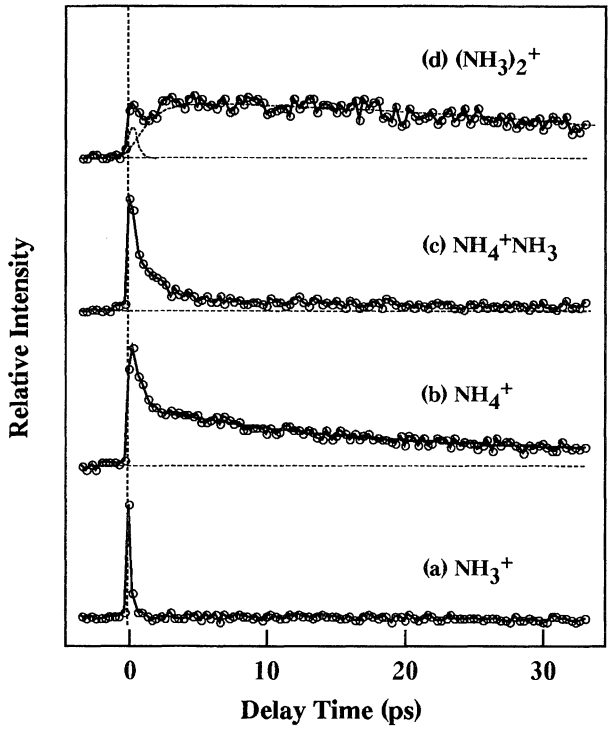

Fig. 4. Pump-probe curves of NH_3^+ (a), NH_4^+ (b), $NH_4^+NH_3$ (c), and $(NH_3)_2^+$ (d) with a scan step of 330 fs; pump pulses at 197 nm, A ($v_2'=5$), and probe pulses at 263 nm. All signals, except for NH_3^+, do not fall back to the background level. The intracluster reactions, which form the long-lived clusters containing NH_4, are responsible for these signals.

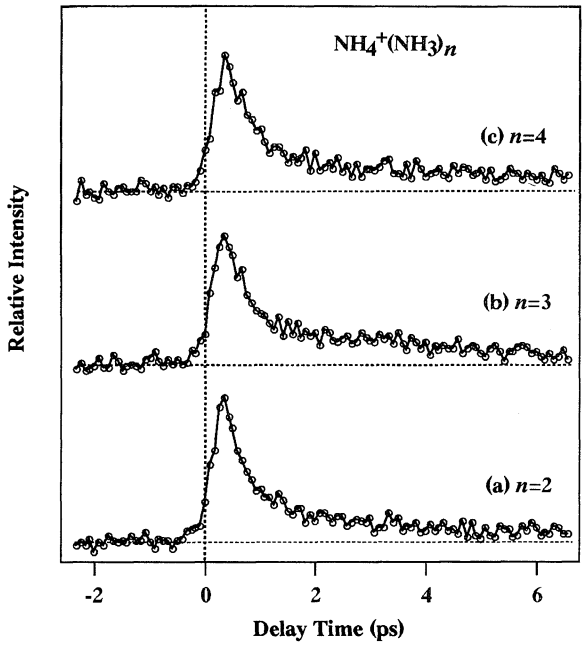

Fig. 5. Pump-probe curves of $NH_4^+(NH_3)_n$, n=2—4, with a scan step of 83 fs; pump pulses at 197 nm, A ($v_2'=5$), and probe pulses at 263 nm.

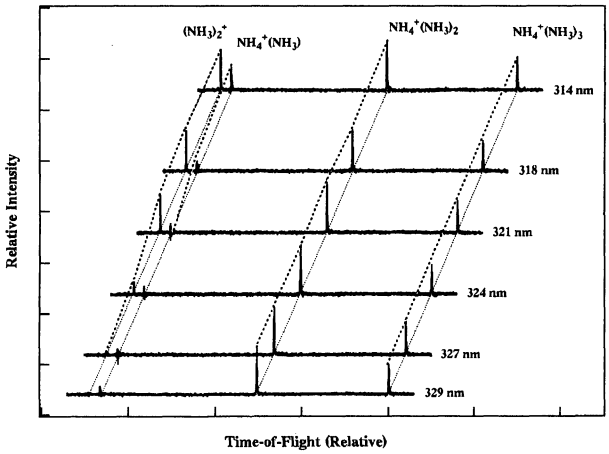

Fig. 6. Typical TOF mass spectra of small ammonia cluster ions generated by two nanosecond laser pulses with zero delay time; pump pulses at 212.8 nm, A ($v_2'=1$), and probe laser in the wavelength region of 329—314 nm. $(NH_3)_2^+$ and $NH_4^+NH_3$ exhibit threshold behaviors with appearance energies of 3.79 and 3.88 eV, respectively.

of NH_4^+ may be responsible for the decomposition process of NH_4. Assuming a single exponential decay, the lifetime of NH_4 is estimated to be 13±2 ps.

As shown in Fig. 2, unprotonated ions, $(NH_3)_n^+$, are also formed when the pump and probe pulses are temporally overlapped: the ion signals for $n>2$ decrease rapidly with increasing the delay time, as in the case of NH_3^+. On the other hand, the unprotonated dimer ion shows a unique time response; the pump-probe curve of $(NH_3)_2^+$ consists of a rather weak spike and a rising curve, as schematically shown by the dotted lines in Fig. 4d. The former component may correspond to ion signals due to the RE2PI process, while the latter component indicates the existence of an intermediate species which is one-photon-ionized by the 263 nm pulse to form $(NH_3)_2^+$. To obtain further information concerning the intermediate, we carried out the two-color photoionization experiments with nanosecond laser pulses. The fifth harmonic of a Nd : YAG laser at 212.8 nm, which corresponds to the A state ($v_2'=1$) of the ammonia molecule, was used as the photolysis laser. On the other hand, the second harmonic of the excimer-pumped dye laser was used as the probe laser with zero delay time. Figure 6 shows typical TOF mass spectra of small ammonia cluster ions produced at various probe-laser wavelengths (329—314 nm, 3.77—3.95 eV). The ionization efficiency of $NH_4(NH_3)_n$ (n=2, 3) does not change appreciably in this wavelength range, while that of $NH_4^+(NH_3)$ exhibits a threshold behavior: Note that the weak signals below the threshold wavelength (ca. 321 nm) for the latter ion are from one color ionization by the pump laser. These results are consistent with those obtained in our previous photoionization study; the ionization thresholds of $NH_4(NH_3)_n$ (n=1—3) were determined to be 3.88, 3.31, and 2.97 eV, respectively.[28] On the other hand, the ionization

efficiency of $(NH_3)_2^+$ decreases rapidly from 321 to 329 nm (3.862—3.768 eV) and gives the threshold energy of the intermediate as 3.79 eV.

In order to obtain further insight into the mechanism of the stabilization of NH_4 in clusters, we also measured the lifetime of $NH_4(NH_3)_n$ using the pump-probe technique with nanosecond lasers. Since long-lived photolysis products are drifted downstream with time in a molecular beam, it is difficult to probe the concentration quantitatively using a probe beam with a small beam diameter. To suppress the loss of clusters in the ionization region, a top-flat laser beam with a large cross section is required. For this purpose, we used a far-field beam of an XeCl excimer laser at 308 nm as the probe pulses; the width and height of the beam were ca. 15 and 5 mm, respectively. The uniformity of the laser fluence was examined by moving a power meter with a 0.5-mm-width slit across the cross section of the probe laser. The averaged fluctuation of the probe laser was estimated to be less than ±5%, as shown in Fig. 7. To correlate the width of the probe beam with time, we also measured the time-of-flight of the photolysis product. The figures inserted in Fig. 7 show the experimental configuration and the velocity distribution of $NH_4(NH_3)_6$, which is expected to have a dissociation lifetime of >20 μs. In the velocity-distribution measurements, a probe beam with a cross section of 1×5 mm was sent to the center of the acceleration region of the mass spectrometer, while a pump laser beam with a 1 mm diameter was introduced colinearly 5 mm upstream with regard to the probe beam. The distribution was measured by detecting the ion signals as a function of the delay time between the pump and the probe lasers. The average velocity of $NH_4(NH_3)_6$ in the molecular beam was estimated to be 1130 $m\,s^{-1}$. Thus, the effective width of the probe beam (13 mm) corresponds to that of a time window of ca. 12 μs. Figure 8 shows the pump-probe curves for $NH_4^+(NH_3)_n$ (n=1—3, 5). With increasing the delay time, the clusters are ionized at the lower reaches of the stream in the acceleration region, and, as a result, the resolution of the mass spectrum changes significantly in the present time window. Therefore, the integrated intensity for each mass peak is plotted in Fig. 8 (open circles) as a function of the delay time. We must also consider an effect of the metastable decay of $NH_4^+(NH_3)_n$ on the observed decay curves. The unimolecular dissociation of these ions has been studied extensively using the reflectron TOF mass spectrometer; these studies predicted that the extent of dissociation increases with cluster size.[30] If this process occurs efficiently in the first field-free region of the reflectron, the decay curve examined should be distorted, especially for large clusters. However, the metastable fractions for $n\leq4$ were found to be negligible, and also, the fractions for n=5 and 6 were less than 10% under the present experimental conditions. Also, in the lifetime measurements of each cluster, the TOF in the first field-free region is almost the same for the ions produced at different delay times. Therefore, the observed decay curves for $n\leq5$ shown in Fig. 8 may not be seriously affected by the metastable decay process. As can be seen in the figure, the observed data for n=1 and 2 were fitted reasonably in a single exponential function, from which the decomposition lifetimes are determined to be 3±1 and 7±2 μs, respectively. On the other hand, the larger clusters have lifetimes longer than 10 μs, and drift out from

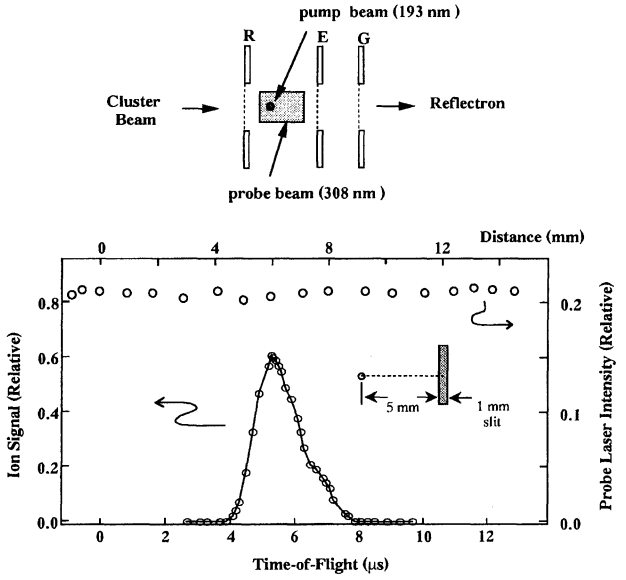

Fig. 7. Schematic configuration of pump-probe experiments for $NH_4(NH_3)_n$ (upper case). Time-of-flight of $NH_4(NH_3)_6$ and laser intensity at different portion of the probe beam (lower case, see text).

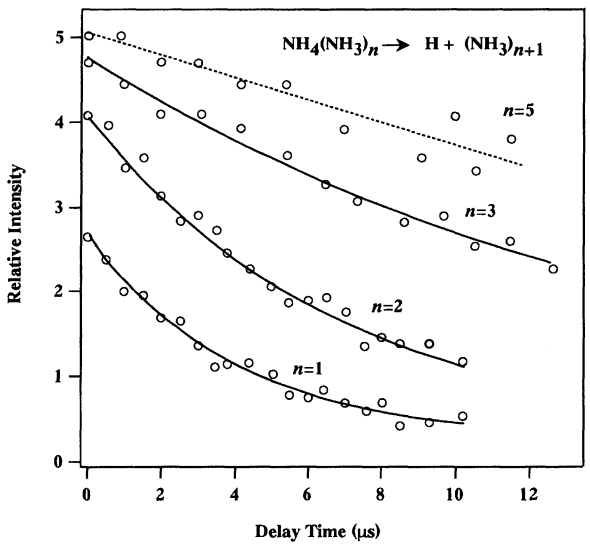

Fig. 8. Pump-probe curves of $NH_4^+(NH_3)_n$, n=1—3 and 5; pump pulses at 193 nm and probe pulses at 308 nm. Clusters with $n\geq3$ have a lifetime of longer than 10 μs and drift out from the time window.

the present time window of the probe beam as shown in Fig. 8. These results as well as those for the femtosecond experiments clearly indicate that the lifetime of NH_4 is elongated by more than 10^6 times in clusters.

Discussion

The photoionization of ammonia clusters has been known to produce protonated cluster ions predominantly both in the one-photon ionization and RE2PI process via the first excited state.[4—10] As for the formation of these ions in the latter process, two mechanisms, such as the AID,

$$(NH_3)_n + h\nu_1 \rightarrow (NH_3)_n^* + h\nu_2 \rightarrow (NH_3)_n^+ \rightarrow NH_4^+(NH_3)_{n-2} + NH_2 \quad (1)$$

and ADI processes were proposed on the basis of the theoretical calculations.[12,13] The latter mechanism is considered to include the following dynamical processes:

$$(NH_3)_n + h\nu_1 \rightarrow (NH_3)_n^*(A) \quad (2)$$

$$(NH_3)_n^*(A) \rightarrow (NH_3)_{n-2}\cdot NH_4^* \cdots NH_2 \quad (3)$$

$$(NH_3)_{n-2}\cdot NH_4^* \cdots NH_2 \rightarrow (NH_3)_{n-2}\cdot NH_4 + NH_2 \quad (4)$$

$$NH_4(NH_3)_{n-2} + h\nu_2 \rightarrow NH_4^+(NH_3)_{n-2} \quad (5)$$

Here, $NH_4^*\cdots NH_2$ is an excited-state NH_4–NH_2, as discussed later. Process 3 corresponds to the predissociation of ammonia molecules to form clusters containing $NH_4^*\cdots NH_2$, while process 4 corresponds to the formation of NH_4 in clusters. The competing process between the AID and ADI mechanisms to form protonated ions in RE2PI were supported by the recent studies using nanosecond lasers.[9,10] More recently, Castleman and co-workers carried out femtosecond RE2PI experiments to reconfirm these two mechanisms.[16,17] The latter authors examined the formation process of $NH_4^+(NH_3)_n$ ($n=1$—4) via the $v_2'=0$—2 levels in the first excited state. In the present study we reexamined the RE2PI process via the A ($v_2'=5$) state to gain further insight into the photochemistry of ammonia clusters on the excited-state surface as well as the cluster-size dependence for the formation and decomposition processes of $NH_4(NH_3)_n$.

(I) Predissociation of $(NH_3)_n(A)$ and Formation of Ammoniated NH_4. The mechanism of the photodissociation of ammonia following excitation to its first excited state has been extensively studied.[14,15,31—33] Before discussing the results on clusters, it is worth briefly summarizing the features for the photodissociation dynamics of an ammonia molecule in the A state. In a free molecule, an energy barrier of ca. 0.4 eV along the predissociation coordinate was predicted theoretically.[31] The dissociation of NH_3 in the lower bending vibrational levels is considered to take place through a quantum mechanical tunneling of this barrier. The topology along this dissociation coordinate is complicated at a larger H–NH_2 distance due to the presence of a conical intersection between the X- and A-state surfaces of NH_3. The product state distribution has been extensively examined by Ashfold and co-workers using a H-atom photofragment translational spectroscopy.[32,33] According to their results, the dissociation yields primarily the ground-state NH_2 fragments, but with high levels of rotational excitation about the a-inertia axis. For the lower v_2' excitation, dissociation from those levels with even quanta yields a much greater proportion of fragments in low rotational quantum states, while those with odd quanta yield $NH_2(X)$ fragments with substantially higher levels of a-axis rotational excitation. They also estimated the partition of available energy in $NH_3(A)\rightarrow NH_2(X)+H$ ($E_{avl}=1.08-1.64$ eV for $v_2'=0$—5). The results indicate a rather small v_2' dependence of energy disposal for the H-atom fragment kinetic energy (0.55 eV and 0.35 eV for $v_2'=0$ and 5, respectively).[33] These features concerning the dissociation dynamics of NH_3 may to some extent reflect those for clusters. In the following paragraphs we first discuss the formation process of the protonated cluster ions, and then discuss that for the unprotonated cluster ions.

As shown in Fig. 3a, the pump-probe curve of NH_3^+ exhibits a nearly symmetric peak with the zero base line. These features indicate that the NH_3^+ ions are mainly produced by the ionization of free NH_3 molecules, and that the contribution of fragment ions from larger clusters is negligible within the experimental error: The pump pulses at 197 nm excite NH_3 to the first excited state, while the probe pulses ionize the electronically excited ammonia. The FWHM of the peak (ca. 370 fs) is close to that for the cross-correlation function of the pump and probe pulses. This result is consistent with an ultrafast predissociation rate of the A ($v_2'=5$)-state ammonia ($>1/100$ fs).[14] Needless to say, it is indispensable to define the zero of the time of the experimental system to examine the cluster-size dependence of the time evolution of the ions, the time when the overlap between the pump and probe pulses is maximal. However, it is rather difficult to determine the zero of the time because of the lack of a suitable internal reference. Since the NH_3^+ ions exhibit an ultrafast response, as mentioned above, the zero of the time was approximated to the peak of the NH_3^+ ion signals; the present $t=0$ is quite close to the true one, but not the exact one. As shown in Fig. 3c, the pump-probe curve of $NH_4^+(NH_3)$ shows two decay components, such as a large increase in intensity, and, thereafter, a rapid intensity drop, followed by a second slower decay to a non zero value of intensity. The peak of $NH_4^+(NH_3)$ shifts to the longer delay time with respect to $t=0$. This feature as well as the rapid decay (<0.5 ps) of the first component suggests that the spike is attributable to signals formed by the AID mechanism. The rapid decay indicates the occurrence of a fast predissociation process in the A ($v_2'=5$) state. With increasing n, the

time to reach the maximum is further delayed, as shown in Figs. 3 and 5. Also, the decay time of the fast component is seen to be elongated for larger clusters. These results may suggest a slowing of the predissociation rate with increasing n. Similar trends were also observed in the pump-probe curves for the excitation at lower v_2' by Castleman and his co-workers.[16,17] However, they did not define the zero of the time properly, and, thus, we cannot directly compare the present results with theirs.

As can be seen in Fig. 4c, the slower decay component of $NH_4^+NH_3$ levels off to a non-zero value of intensity for a delay time longer than ca. 5 ps. Since $NH_4(NH_3)_n$ ($n \geq 1$) have long lifetimes (≥ 3 μs), as shown in the next section, and have ionization threshold energies lower than the probe-laser energy (263 nm),[28] the signals of the protonated ions in $\Delta t > 5$ ps are ascribed to those formed by the one-photon ionization of $NH_4(NH_3)_n$; the solvation of NH_4 (process 4) is expected to be nearly completed in this time region. On the other hand, the slow-decaying component in 1 ps$< \Delta t <$5 ps may correspond to process 4. According to the theoretical calculations by Kassab, et al.,[12] the predissociation of $(NH_3)_2^*$ to produce NH_4 (processes 3 and 4) releases an excess energy of ca. 0.9 eV. Most of this energy may be removed by NH_2 fragments in a dimer, as in the case of free molecule mentioned above. For larger clusters, the amount of excess energy released may be greater than that of a dimer, because an excess energy is also generated upon solvation of NH_4; thus, nascent clusters containing NH_4 may be substantially hot. Since the barrier height of the H-atom migration in ammonia clusters is substantially low (as mentioned later), the nascent H-atom trapped may migrate inside of the clusters. Some of them loose kinetic energy through an intracluster vibrational relaxation process to form a stable ammoniated NH_4, though most of them may leave from the clusters. These processes are considered to reflect the slow decaying signals in 1 ps$< \Delta t <$5 ps. These processes may also include an evaporation of ammonia molecules, which makes a quantitative analysis of the observed curves difficult; the observed decay curve may consist of multiple exponential functions. Because of this reason, we did not make any attempt to convolute the curve to reduce the time constant; however, the ratio between the height of the first peak and the non-zero value in $\Delta t > 5$ ps may give a measure of the quantum efficiency of $NH_4(NH_3)_n$ production.

As for NH_4^+, the rapid-decay component is also followed by slow decaying signals, which decay at a much slower rate than those for the slow component of its clusters. These results indicate that NH_4 seems to be formed within $<$0.6 ps; NH_4 is expected to be formed mainly from the ammonia dimer, and the excess energy generated in the predissociation process may be removed by NH_2 fragments at a much faster rate than those for the clusters. On the other hand, NH_4 has been known to be decomposed into NH_3+H, and has an estimated lifetime of $<$100 ps.[23] Thus, the slow-decaying component of the NH_4^+ ion signals is reasonably ascribed to the decomposition of NH_4. Assuming a single exponential decay, the lifetime of NH_4 is determined to be 13±2 ps. In the next section we discuss this result in more detail.

Except for $n=2$, unprotonated ions are not observed in RE2PI with nanosecond lasers, as shown in Fig. 6. On the contrary, $(NH_3)_n^+$ are weakly observed in pump-probe experiments with femtosecond laser pulses. However, these ions are observed only when the pump and probe pulses are temporally overlapped (except for $n=2$ as shown in Fig. 2). The unique features for the formation of $(NH_3)_2^+$ were also pointed out without any definitive interpretation by Nishi, et al.[10] and Castleman, et al.[17] in nanosecond and femtosecond photoionization studies, respectively. In order to clarify the mechanism for the formation of this ion, we measured the pump-probe curves, as shown in Figs. 3d and 4d. The temporal profile exhibits a weak spike superimposed on rising signals. In analogy with the above discussions, the spike may correspond to ion signals generated through the AID process of ammonia dimer. On the other hand, the latter signals increase up to a delay time of ca. 5 ps, and, thereafter, decrease with a much slower decay time; a preliminary pump-probe experiment with nanosecond lasers gives a decay time of $<$1 ns. This feature indicates that a new intermediate, which is one-photon ionized at 263 nm to produce $(NH_3)_2^+$, is formed by the pump laser at 197 nm. This ion is also found to be detected in nanosecond pump-probe experiments with the pump wavelength at 212.8 nm, and has an appearance energy of 3.79 eV as shown in Fig. 6. The appearance energy obtained by using an ArF excimer laser at 193 nm as the pump laser agrees with the above value. Misaizu and co-workers have also crudely estimated the upper limit of the ionization energy as being 3.99 eV, and assigned the intermediate to the excited-state ammonia dimer [$(NH_3)_2^*$ in process 2].[10] However, their assignment is inconsistent with the present results; if the intermediate is $(NH_3)_2^*$, we could see no rising feature, as shown in Fig. 3d. Hence, the observed feature suggest us to consider an alternate candidate. Fortunately, Kassab and co-workers,[12] and recently, Iwata and co-workers,[13] have carried out calculations for the proton-(hydrogen-) transfer surfaces in $(NH_3)_2^+$ and $(NH_3)_2^*$. They predicted that $(NH_3)_2^+$ has no local minimum, and rearranges without a proton-transfer-barrier to give NH_4^+–NH_2. Iwata's group also found that $(NH_3)_2^*$ has a shallow minimum, but that it readily rearranges to NH_4^*–NH_2.[13] Here, the latter species is an excited-state NH_4–NH_2 on the reaction pathway of $(NH_3)_2^*$ to $NH_4+NH_2(^2B_1)$, which is an A″ pathway in C_s symmetry. According to the calculations,[12] the complexation energies for NH_4^+–NH_2 and NH_4^*–NH_2 are 1.07 and 0.32 eV, respectively, while the adiabatic ionization

potential (IP) of NH_4 is 4.66 eV. From these values, the adiabatic IP of NH_4*–NH_2 is calculated to be 3.91 eV, which is close to the observed appearance energy of $(NH_3)_2^+$ (3.79 eV). As for NH_4–NH_2, Iwata and coworkers have predicted that the ground-state NH_4–NH_2 has no local minimum, and dissociates into two ammonia molecules without an energy barrier.[34] Hence, these results as well as the observation, that the intermediate has a lifetime of less than 1 ns, seem to support the assignment of the intermediate as the excited-state NH_4–NH_2 (hereafter abbreviate as NH_4*–NH_2). They also pointed out that there are at least four low-lying excited states which give $NH_4(3p)+NH_2(^2B_1)$ and $NH_4(3s)+NH_2(^2A_1)$ at the asymptote, and that these states and the aforementioned excited state are to some extent mixed with each other. Therefore, an elaborated theoretical calculation is indispensable to assign the observed intermediate definitively. It is worth noting that the ionization efficiency of $(NH_3)_2^+$ increases rapidly above the threshold as shown in Fig. 6. This result indicates that the geometry of the initial state is similar to that of the ionization state. The observed adiabatic ionization is also compatible with the theoretical expectations; NH_4*–NH_2 has an electronic structure of the Rydberg nature, and its geometrical structure may be close to that of NH_4^+–NH_2.

The above assignment seems to provide new insight into the photodissociation mechanism of ammonia clusters in the A state. The predissociation of ammonia molecules generates both the H atom and the NH_2 radical in clusters. The H atom is trapped rather efficiently in ammonia clusters. The high trapping efficiency of the H atom is due to the fact that NH_4 formed in the intracluster reaction is semi-ionic, and binds to NH_3 with a fairly large binding energy (0.34 eV) as mentioned in the next section.[28] On the other hand, neutral clusters containing NH_2 and ion clusters, such as $NH_2(NH_3)_m^+$, are rarely detected (see Figs. 2 and 6), because the IPs of NH_2 and $(NH_3)_n$ are much higher than the energy of the probe laser at 263 nm.[4,35] The other possible reason for the hard detection of the neutral clusters may be due to the low trapping efficiency of NH_2 in ammonia clusters. The nascent NH_2 fragments are expected to have a high internal energy, as in the case of the free molecule mentioned previously. Also, the bonding between NH_2 and NH_3 may be much weaker than that for NH_4–NH_3.[12] These factors may make it difficult for NH_2 to remain in $(NH_3)_m$ after photolysis. In contrast to these arguments, the above assignment for NH_4*–NH_2 suggests that both the H atom and the NH_2 radical are confined within clusters under certain circumstances. As for larger clusters, an electric deflection study supports a cyclic structure in the ground state.[2] If this structure is retained in the A state (vertical transition), even one of the ammonia molecules takes place the predissociation, the other molecules may attract the fragments (H and NH_2) to each other and prevent them from fragmentation; the other molecules may play the role of a cage. The slow rise time of $(NH_3)_2^+$ seems to indicate that it is generated through the photolysis of substantially large clusters.

As mentioned previously, only $(NH_3)_2^+$ is detected in nanosecond experiments. Moreover, in femtosecond experiments, $(NH_3)_n^+$, $n>2$, are detected only when the pump and probe pulses are nearly overlapped in time. These observations are consistent with each other, and may indicate that the precursor, such as $(NH_3)_{n-2}NH_4$*–NH_2, $n>2$, has a lifetime as short as <1 ps. The possible reason for the fast decomposition of these clusters may be due to the nature of the ground- and excited-state surfaces of NH_4–NH_2. As is expected from the predissociation of NH_3 to NH_2+H, the reaction pathway of $(NH_3)_n$* to $NH_4(NH_3)_{n-2}+NH_2(^2B_1)$ mentioned previously shows a strong avoided crossing, originating from a conical intersection known in the ground-state surface of NH_3 to NH_2+H. Therefore, a nonadiabatic transition to the unstable ground state may be strongly enhanced upon complex formation due to these features for the potential energy surfaces as well as the ionic character of NH_4*–NH_2.

The above arguments suggest that, though the excited-state $(NH_3)_{n-2}NH_4$*–NH_2 may be formed in photolysis as in the case of NH_4*–NH_2, it rapidly rearranges to ammonia clusters via an internal conversion (IC) process. If this is the case, in RE2PI with femtosecond lasers, the IC process may compete with the ionization of $(NH_3)_{n-2}NH_4$*–NH_2 by probe pulses to form $(NH_3)_n^+$. Hence, it is necessary to consider that $(NH_3)_n^+$ [i.e. $(NH_3)_{n-2}NH_4^+$–NH_2] is formed through both the ADI and AID mechanisms as shown in Fig. 9. The formation ratio of unprotonated ions via these two mechanisms depends on the IC rate of $(NH_3)_{n-2}NH_4$*–NH_2 and the rate of ionization (i.e. the fluence of the probe laser). In fact, the ADI mechanism operates dominantly for the production of $(NH_3)_2^+$ as can be seen in Fig. 2. For $(NH_3)_n^+$ ($n>2$), both the ADI and AID mechanisms may take part in the forma-

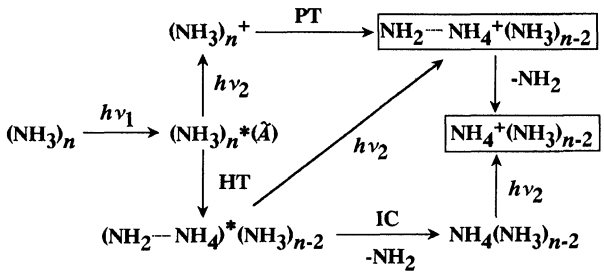

Fig. 9. Possible schemes for the production of unprotonated and protonated cluster ions in the resonance enhanced two-photon ionization through the A-state of ammonia clusters. PT; proton-transfer reaction without an energy barrier. HT; hydrogen-transfer reaction. IC; internal conversion followed by the dissociation of NH_2.

tion of these ions.

(II) Stability of $NH_4(NH_3)_n$. The potential energy surface of the ground-state NH_4 has been examined theoretically by several authors.[34,36,37] These studies have predicted that the radical has a very shallow well in the ground state, which arises from an avoided crossing between the potential curves of the 3s state of NH_4 and the valence-shell repulsive state of NH_3+H. Porter and co-workers examined the stability of NH_4 by a neutralized ion-beam technique and estimated the lifetime as being less than 150 ns.[24] The present result (13±2 ps) is much shorter than their estimation and is consistent with the observed diffused feature of the NH_4 Schüler band.[23] The latter authors also determined the heat of reaction ($NH_4 \rightarrow NH_3+H$) as being 0.103 eV from measurements of the kinetic energy released in the H-atom fragments. They also estimated the barrier height along the dissociation coordinate as being 0.41±0.7 eV. On the other hand, Kaspar and co-workers[36] calculated the potential energy surface having a barrier height of 0.64—0.75 eV, which agrees rather well with the above experimental result. These authors also predicted that there exists only one quasibound vibrational level ($v''=1$) with a lifetime of 2 ps for NH_4; dissociation from $v''=0$ is endothermic and may not take place. However, the result concerning the lifetime, as well as that for the heat of reaction mentioned above, indicate the metastability of NH_4 and seems to be inconsistent with their predictions.

As for $n=1$ and 2, the lifetimes were determined to be 3±1 and 7±2 μs as shown in Fig. 8. Gellene and co-workers also estimated the lifetime of $NH_4(NH_3)$ as being >0.96 μs,[25,26] which is compatible with the present results. Thus the lifetime is elongated by more than 10^6 times due to complex formation. In a previous study we determined the ionization potentials of $NH_4(NH_3)_n$ from the measurements of the ionization efficiency curves.[28] Using these IP results and the successive binding energies ($\Delta H_{n-1,n}$) for $NH_4^+(NH_3)_n$, determined by equilibrium mass spectrometry measurements,[38,39] we estimated the binding energies ($D_{n-1,n}$) of the ammoniated radicals. As for $n=1$, Kebarle and his co-workers[38] determined $\Delta H_{0,1}$ as being 1.08 eV, while Futrell's group[39] reported a value of 0.93 eV. From these values and the IP of $n=1$ (3.88 eV),[28] $D_{0,1}$ is estimated to be 0.34 and 0.19 eV, respectively. These values are much larger than the dissociation energy of the ammonia dimer [<0.12 eV[40]], and indicate that the bonding between NH_4 and NH_3 is semi-ionic, as predicted theoretically by Kassab and Evleth.[27] Since the reaction $NH_4 \rightarrow NH_3+H$ is nearly isoergic [$\Delta H=0.103$ eV[24]], the significantly larger binding energy of NH_4 with NH_3 comparing with NH_3 itself may cause a decrease in the heat of reaction, and as a result, the reaction is suppressed as schematically shown in Fig. 10. From these arguments, the reaction of NH_4NH_3 is expected to be almost endothermic; the heat of reaction is estimated to be −0.12—0.03 eV. However, the result on the lifetime for $n=1$ (3 μs) seems to suggest that the reaction is still exothermic. For $n=2$—6, the successive binding energies ($D_{n-1,n}$) were estimated to be 0.12, 0.26, 0.30, 0.24, and 0.14 eV, respectively.[28] The reason why $D_{1,2}$ is so small compared with its neighbor is not clear at present, however, the small binding energy is consistent with the relatively short lifetime of $n=2$; the lifetime is elongated only by a factor of two upon complexation with the second ammonia molecule. Since $D_{1,2}$ is close to that for the ammonia dimer, the exothermicity of $n=2$ and the rate of decomposition as well is expected to be close to those for $n=1$. According to the calculations,[27] the optimal structure of $NH_4(NH_3)_4$ is C_{3v}; four NH_3 molecules ligate to H atoms in NH_4 and form the first solvent shell, as in the case of $NH_4^+(NH_3)_4$. The rather rapid decrease in $D_{n-1,n}$ from $n=4$ to 6 seems to support these theoretical predictions. In the calculations, they implicitly assumed that the excess H atom is localized on one ammonia molecule surrounded by the other NH_3 molecules. If this is the case, the clusters with $n \geq 4$ may be stable. Contrary to this expectation, $NH_4^+(NH_3)_5$ has a finite lifetime as shown in Fig. 8. This fact may imply that the excess H atom in clusters is partially delocalized in clusters, because the clusters are substantially hot due to the large binding energy. To confirm this possibility, an accurate measurement of the lifetime for larger clusters is underway in this laboratory.

Conclusions

This paper describes the results of investigations concerning the formation and decay processes of clusters containing the NH_4 radical produced in the predissociation of the A ($v_2'=5$)-state ammonia clusters. The clusters produced by photolysis were detected by the pump-probe technique with nanosecond and femtosecond lasers. Although the predissociation rate in the A-

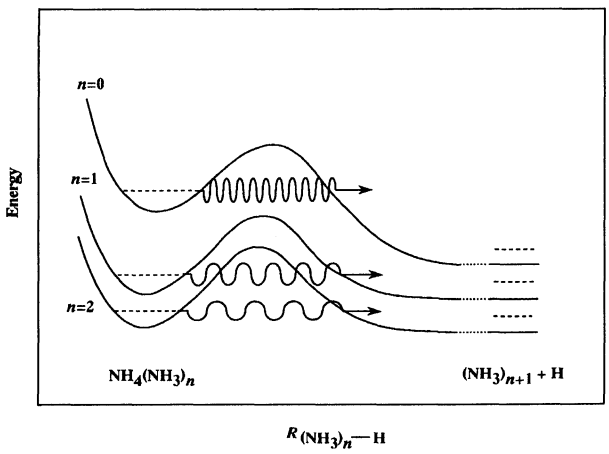

Fig. 10. Schematic illustration for the stabilization mechanism of NH_4 in ammonia clusters.

state ammonia clusters is reduced with increasing n, it is completed within 1 ps even for $n \geq 4$. The unique time profile of $(NH_3)_2^+$ is ascribed to the formation of a new intermediate, which forms an ammonia dimer ion through one-photon ionization with the probe laser. On the basis of the result of the IP measurement as well as those of the theoretical calculations, the intermediate has been identified as the excited-state NH_4^*–NH_2. The rise time of this species indicates that it is formed through cage dynamics due to the predissociation of large ammonia clusters. These findings give new insight into the photochemical reaction dynamics of ammonia clusters in the A state. Also, the results suggest a new mechanism for the production of unprotonated ions such as the ADI mechanism. This mechanism seems to play an important role in resonance enhanced MPI with ultrafast laser photons.

The decomposition lifetime of NH_4 was determined to be 13 ps, while that for NH_4NH_3 was found to be 3 μs. Although the lifetimes of larger clusters are longer than 10 μs, that for $n=5$ is finite. Thus the lifetime of NH_4 is elongated by more than 10^6 times in clusters. The huge stabilization is ascribed to the semi-ionic character of the NH_4 radical. Since $NH_4(NH_3)_n$ is expected to be rather hot, and the energy barrier of H-atom migration in clusters is substantially low, the excess H atom may be to some extent delocalized over the cluster. The fact that the lifetime of $n \geq 4$ is finite may support this possibility.

The authors would like to thank Professor S. Iwata and Dr. J. K. Park for valuable discussions and Mr. Yamanaka for his technical assistance. The financial support from Grant-in-Aids for Scientific Research for Priority Area No. 07240102 from the Ministry of Education, Science and Culture is greatly acknowledged.

References

1) W. Kamke, in "Cluster Ions," ed by C. Ng, T. Baer, and I. Powis, John Wiley & Sons, New York (1993), Chap. 1.

2) J. A. Odutola, T. R. Dyke, B. J. Howard, and J. S. Muenter, *J. Chem. Phys.*, **70**, 4884 (1979).

3) K. Stephan, J. H. Futrell, K. I. Peterson, A. N. Castleman, Jr., H. E. Wagner, N. Djuric, and T. D. Mark, *Int. J. Mass Spectrom. Ion Phys.*, **44**, 167 (1982).

4) S. T. Ceyer, P. W. Tiedemann, B. H. Mahan, and Y. T. Lee, *J. Chem. Phys.*, **70**, 14 (1979).

5) H. Shinohara, N. Nishi, and N. Washida, *J. Chem. Phys.*, **83**, 1939 (1985).

6) E. Kaiser, J. de Vries, H. Steger, C. Menzel, W. Kamke, and I. V. Hertel, *Z. Phys. D*, **20**, 193 (1991).

7) H. Shinohara and N. Nishi, *Chem. Phys. Lett.*, **87**, 561 (1982).

8) O. Echt, P. D. Dao, S. Morgan, and A. N. Castleman, Jr., *J. Chem. Phys.*, **82**, 4076 (1985).

9) F. Misaizu, P. L. Houston, N. Nishi, H. Shinohara, T. Kondow, and M. Kinoshita, *J. Phys. Chem.*, **93**, 7041 (1989).

10) F. Misaizu, P. L. Houston, N. Nishi, H. Shinohara, T. Kondow, and M. Kinoshita, *J. Chem. Phys.*, **98**, 336 (1993).

11) S. Tomoda, *Chem. Phys.*, **110**, 431 (1986).

12) H. Z. Cao, E. M. Evleth, and E. Kassab, *J. Chem. Phys.*, **81**, 1512 (1984).

13) J. K. Park, S. Ten-no, and S. Iwata, private communication.

14) L. D. Ziegler, *J. Chem. Phys.*, **84**, 6013 (1986).

15) K. Fuke, H. Yamada, Y. Yoshida, and K. Kaya, *J. Chem. Phys.*, **88**, 5238 (1988).

16) S. Wei, J. Purnell, S. A. Buzza, and A. N. Castleman, Jr., *J. Chem. Phys.*, **99**, 755 (1993).

17) J. Purnell, S. Wei, S. A. Buzza, and A. N. Castleman, Jr., *J. Phys, Chem.*, **97**, 12530 (1993).

18) J. K. S. Wan, *J. Chem. Educ.*, **45**, 40 (1968).

19) J. M. Brooks and R. R. Dewald, *J. Phys. Chem.*, **75**, 986 (1971).

20) E. Kariv-Miller, C. Nanjundiah, J. Eaton, and K. E. Swenson, *J. Electroanal. Chem.*, **167**, 141 (1984).

21) E. M. Evleth and E. Kassab, *Pure Appl. Chem.*, **60**, 209 (1988).

22) G. Herzberg, *Faraday Discuss. Chem. Soc.*, **71**, 165 (1981).

23) G. Herzberg, *J. Astrophys. Astron.*, **5**, 131 (1984).

24) G. I. Gellene, D. A. Cleary, and R. F. Porter, *J. Chem. Phys.*, **77**, 3471 (1982).

25) G. I. Gellene and R. F. Porter, *J. Phys. Chem.*, **88**, 6680 (1984).

26) S. Jeon, A. B. Raksit, G. I. Gellene, and R. F. Porter, *J. Am. Chem. Soc.*, **107**, 4129 (1985).

27) E. Kassab and E. M. Evleth, *J. Am. Chem. Soc.*, **109**, 1653 (1987).

28) K. Fuke, R. Takasu, and F. Misaizu, *Chem. Phys. Lett.*, **229**, 597 (1994).

29) F. Misaizu, M. Sanekata, and K. Fuke, *J. Chem. Phys.*, **100**, 1161 (1994).

30) S. Wei, W. B. Tzeng, and C. W. Castleman, *J. Chem. Phys.*, **93**, 2506 (1990).

31) M. I. McCarthy, P. Rosmus, H. -J. Werner, P. Botschwina, and V. Vaida, *J. Chem. Phys.*, **86**, 6693 (1987).

32) J. Biesner, L. Schnieder, J. Schmeer, G. Ahlers, Xiaoxiang Xie, K. H. Welge, M. N. R. Ashfold, and R. N. Dixon, *J. Chem. Phys.*, **88**, 3607 (1988).

33) J. Biesner, L. Schnieder, G. Ahlers, Xiaoxiang Xie, K. H. Welge, M. N. R. Ashfold, and R. N. Dixon, *J. Chem. Phys.*, **91**, 2901 (1989).

34) J. K. Park, S. Ten-no, and S. Iwata, to be published.

35) S. T. Gibson, J. P. Greene, and J. Berkowitz, *J. Chem. Phys.*, **83**, 4319 (1985).

36) J. Kaspar, V. H. Smith, Jr., and B. N. MeMaster, *Chem. Phys.*, **96**, 81 (1985).

37) H. Cardy, D. Liotard, A. Dargelos, and E. Poquet, *Chem. Phys.*, **77**, 287 (1983).

38) J. D. Payzant, A. J. Cunnungham, and P. Kebarle, *Can. J. Chem.*, **51**, 3242 (1973).

39) M. R. Arshadi and J. H. Futrell, *J. Phys. Chem.*, **78**, 1482 (1974).

40) D. D. Nelson, G. T. Fraser, and W. Klemperer, *J. Chem. Phys.*, **83**, 6201 (1985).